

# A DOUBLE-PRISM SPECTROMETER FOR THE LONGITUDINAL DIAGNOSIS OF FEMTOSECOND ELECTRON BUNCHES WITH MID-INFRARED TRANSITION RADIATION \*

S. Wunderlich<sup>†</sup>, E. Hass, M. Yan and B. Schmidt, DESY, 22603 Hamburg, Germany

## Abstract

Electron bunch lengths in the sub-10 fs regime and charges of a few tens of picocoulombs are parameters required for free-electron lasers [1] and are also a consequence from the intrinsic process in laser-driven plasma wake field acceleration [2]. Since the coherent spectrum of transition radiation of these bunches carries the information on the longitudinal bunch profile in the form factor, the spectroscopy of transition radiation is an attractive method to determine the electron bunch length. A double-prism spectrometer has been developed and demonstrated for the single-stage measurement of mid-infrared transition radiation between 2 μm and 18 μm. The spectrometer facilitates single-shot spectral measurements with high signal-to-noise ratio utilising a line array of mercury cadmium telluride detectors. In this contribution, we present the spectrometer and measurements of electron bunches at the Free-Electron Laser in Hamburg (FLASH) at DESY. The results are compared to established bunch length monitors which are a multi-stage grating spectrometer for transition radiation and a transverse deflecting structure accessing the longitudinal phase space of the electron bunches directly.

## DIAGNOSIS OF ELECTRON BUNCHES WITH COHERENT RADIATION

The coherent spectrum of characteristic radiation from relativistic and charged particle bunches carries the information on the three-dimensional current profile encoded in the form factor. In other words, the complex form factor  $F$  yields the wavelength-dependent level of coherence in the emission of radiation, like coherent diffraction radiation (CDR), coherent synchrotron radiation (CSR) and coherent transition radiation (CTR). This project focuses on the latter, CTR.

### Spectral Intensity of Coherent Radiation

The spectral intensity  $U = U(\omega, \Omega)$  of transition radiation (TR) per solid angle  $\Omega$  and wavelength  $\omega$  can be described by

$$\frac{d^2U}{d\omega d\Omega} \approx \frac{d^2U_1}{d\omega d\Omega} N^2 |F(\omega, \Omega)|^2 \quad (1)$$

with, expressing the nature of coherent emission, the number of radiating particles squared,  $N^2$ , and the single-particle contribution  $U_1$  [3]. The modulus of the complex form factor is denoted by  $|F(\omega, \Omega)|$ .

\* The project has been supported by the BMBF under contract 05K10GU2 & FS FLASH 301.

<sup>†</sup> steffen.wunderlich@desy.de

## Form Factor

The complex form factor

$$F = F(\omega, \Omega) = |F(\omega, \Omega)| \exp(i\Phi(\omega))$$

is the Fourier transform of the three-dimensional normalised charge density  $\rho_{3D}(\vec{r})$  in position space and can be expressed, at an observation distance much larger than the electron bunch extension, by

$$F(\omega, \Omega) = F(\vec{k}) = \int_{-\infty}^{\infty} \rho_{3D}(\vec{r}) \exp(-i\vec{k}\vec{r}) d\vec{r}.$$

A decomposition of  $F(\omega, \Omega)$  into transverse and longitudinal components,  $F_t$  and  $F_l$ , is justified for a negligible coupling of the two planes [4].

The longitudinal form factor  $F_l = F_l(\omega)$  now reflects a charge density in the direction of the movement of the high-relativistic particles

$$F_l = \int_{-\infty}^{\infty} \rho_l(t) \exp(-i\omega t) dt \quad (2)$$

Due to the high-relativistic motion of the particles, the influence of the transverse form factor is strongly suppressed. This allows to approximate  $F(\omega, \Omega)$  by  $F_l(\omega)$  in Equation (1) for sufficiently small transverse beam sizes [3].

### Utilising $F$ for Estimating the Bunch Length

Figure 1 shows examples of form factors on the beam axis of electron bunches with lengths ( $\sigma_l$ ) in the femtosecond regime between 0.5 μm ( $\approx 1.5$  fs) and 3 μm ( $\approx 10$  fs). As depicted, the form factor shows a strong modulation with bunch length in the wavelength range between 2 μm and 20 μm. Hence, this range has been chosen for the region of interest of the prism spectrometer described in the following section.

According to Equation (2), the determination of the absolute value and the slope of the modulus of the form factor,  $|F_l|$ , allows the estimation of the bunch length and moreover, a time-domain current profile. However, the spectral phase  $\Phi(\omega)$  of the complex form factor  $F$  cannot be acquired by intensity spectroscopy. Underlying several constraints, phase-retrieval processes [5–7] can access a possible temporal current profile and show an impressive accordance with direct time-domain diagnostics like a transverse deflecting structure (TDS) [4].

## DOUBLE-PRISM SPECTROMETER

Compared to grating-based spectrometers, prism spectrometers yield bulk absorption in the prisms, but provide

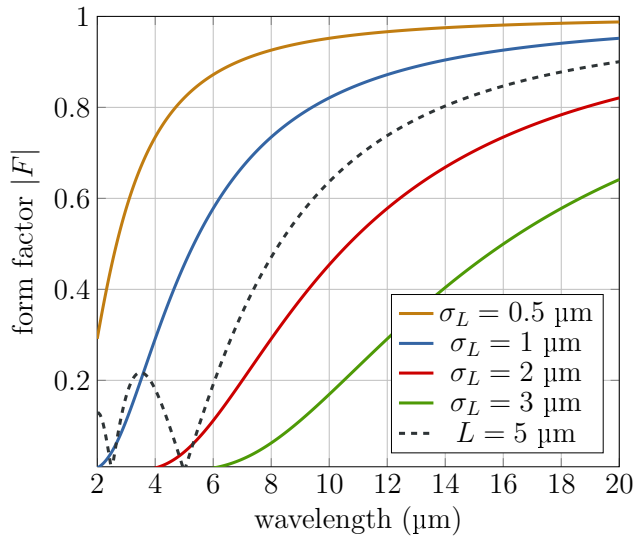


Figure 1: Examples of form factors on the beam axis resulting from a temporal Gaussian shape (*solid*) and rectangular shape (*dashed*) for widths  $\sigma_L$  and total length  $L$ , respectively, in the femtosecond regime.

a continuous dispersion without higher orders. For mid-infrared wavelengths, the polycrystalline compounds *KRS-5*, thallium bromo-iodide, and *zinc selenide* (*ZnSe*) offer a sufficient dispersion at a refractive index  $n > 2.3$ . In contrast to other prism spectrometer setups for beam diagnostics with coherent radiation [8,9], this particular spectrometer utilises an arrangement of two *ZnSe* prisms, as illustrated in Fig. 2, to achieve an integrated linear dispersion in the detector focal plane of approximately 32 mm for the wavelength range between 2  $\mu\text{m}$  and 18  $\mu\text{m}$ .

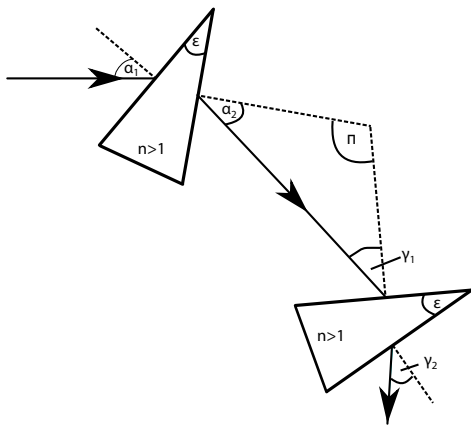


Figure 2: Schematic of the dispersive stage consisting of two consecutive *ZnSe* prisms.

The spectrometer is equipped with a 32 mm-wide line array of 128 mercury cadmium telluride (MCT) photoconductive detector elements [10], which is attached to a liquid nitrogen dewar to preserve a temperature of 77 K for low-noise operation. For mid-infrared wavelengths, MCT detectors yield a signal-to-noise ratio larger by a factor of

ISBN 978-3-95450-141-0

100 compared to pyro-electric radiation sensors utilised in similar spectrometers.

A chain of analogue and digital electronics, including a gated boxcar integrator and a built-in analogue-to-digital converter (ADC), allows a parallel and single-shot data acquisition up to a repetition rate of 50 kHz [11].

### Response Function

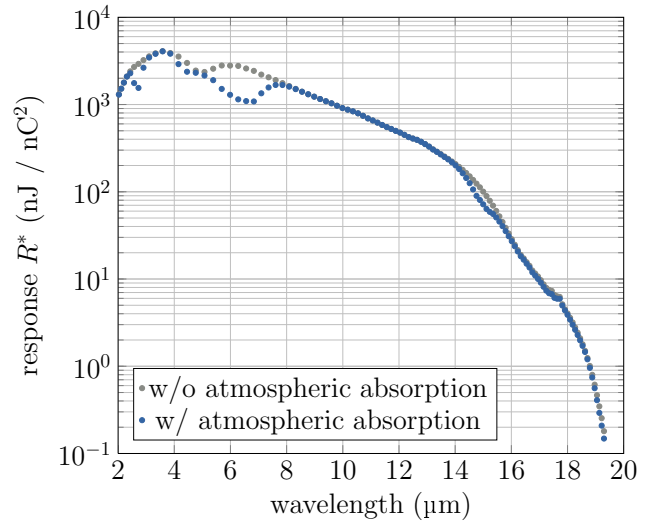


Figure 3: Spectrometer response function  $R^*$ .

The determination of the absolute form factor modulus imposes the knowledge of the so-called *response function*,  $R = a \cdot R^*$ , which expresses the connection of the detector signal, a digitised voltage amplitude, with the absolute TR intensity expected at the detector.

The function  $R^*$  covers the process of imaging of the source, driven by  $N$  particles with elementary charge  $e$ , onto the detector plane and the dispersive process due to the two prisms. In addition, transmissive and reflective losses of the bulk material and the ambient air have been considered. For the latter, data from the HITRAN database [12] have been used.

The response function is depicted in Figure 3, also showing the influence of 3.1 m of ambient air in the free-space beam transport onto the spectrum.

The second important constituent of  $R$  is the absolute intensity calibration  $a$  of the detector unit. The factor  $a = G \cdot R_{\text{abs}}$  provides the conversion of the detector voltage signal  $S$  into an absolute irradiated intensity,  $R_{\text{abs}}$ , in units of Volts/Joules, times a *gain factor*  $G$  accounting for a variable electronic signal amplification.

$$|F| = \frac{1}{N e} \sqrt{\frac{S}{a \cdot R^*}} \quad (3)$$

Since the absolute detector calibration  $a$  is not yet available for mid-IR radiation pulses with pulse durations  $\ll 1$  ns, a cross-calibration with a grating spectrometer with calibrated pyro-electric detectors will be performed. Details

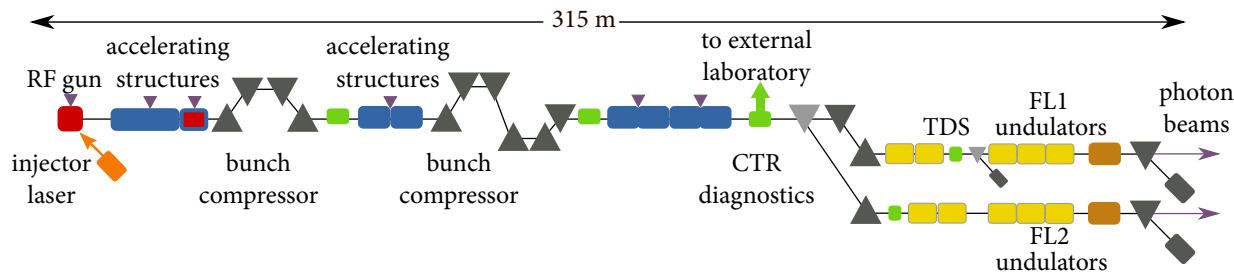


Figure 4: Overview of the FLASH FEL facility with the undulator beamlines FLASH1 (FL1) and FLASH2 (FL2). The locations of longitudinal diagnostics are indicated in *green*. Details can be found in [13].

will be presented later in this contribution. A calibration at an intensity and wavelength standard is in preparation.

## EXPERIMENTAL SETUP

Measurements with the double-prism spectrometer have been taken at the free-electron laser (FEL) facility FLASH, at DESY in Hamburg, Germany [14]. The FLASH linear accelerator provides electron bunch trains with an energy up to 1.2 GeV, charges from a few tens of picocoulombs up to several nanocoulombs and electron bunch lengths down to  $< 50$  fs at a repetition rate of 10 Hz. Due to the superconducting acceleration modules, the bunch trains can consist of a single bunch to 800 bunches at a spacing down to 1  $\mu$ s.

The transition radiation source, consisting of a aluminium-coated silicon screen, is located at the end of the linac. The transverse beam size is approximately 200  $\mu$ m (Gaussian,  $1\sigma$ ). The TR is guided into an external laboratory [15], where the double-prism spectrometer is accessible independently from the operation of the FEL. The beam transport line is kept in vacuum and sealed towards the spectrometer setup by a 3 mm thick zinc selenide window.

At the TR source, also a calibrated multi-stage grating spectrometer [3], CRISP4, is available. The dispersive section consists of two sets of four consecutive gratings spanning the wavelength range between (5 – 44)  $\mu$ m and (45 – 430)  $\mu$ m, respectively. The pyro-electric detectors utilised in the CRISP4 spectrometer are calibrated absolutely. As reported in [3] and [4], the measured form factors  $|F|$  are in striking agreement with the transverse deflecting structure.

Referring to Figure 4, the transverse deflecting structure (TDS) at FLASH is located in front of the SASE undulators in the FLASH1 beamline, separated from the CTR source by electron beam transport and a dispersive section for energy collimation [16]. The TDS is a LOLA-type RF cavity [17] and offers a direct access to the time-domain current profile and the longitudinal phase space by streaking the bunch transversally, i.e. translating the longitudinal plane into a transverse plane, in combination with a dipole spectrometer.

## MEASUREMENTS

The measurements presented in this section have been acquired in May 2014 complementary to studies of the CRISP4 spectrometer and the TDS.

Figures 5 and 6 depict the form factor modulus  $|F|$  of measurements with the CRISP4 spectrometer and the double-prism spectrometer for two compression settings. The data of the latter diagnostic have been scaled according to Equation (3). The scaling factor,  $a$ , normalised to the maximum electronic gain, has been calculated for the two settings to  $(31.66 \pm 0.40)$  V/nJ and  $(38.24 \pm 0.76)$  V/nJ. The uncertainty denote the r.m.s. deviation from the mean of 1000 and 500 single shots respectively.

The form factors of the two spectrometers show a significant accordance in the range between 8.5  $\mu$ m and 13.5  $\mu$ m, which has been used to determine the scaling factor  $a$ . The striking similarity in the slope of  $|F|$  and the values of  $a$  for the two settings within one standard deviation indicate an attractive performance of the prism spectrometer in comparison to the calibrated and established CRISP4. For these measurements, the peak signal-to-noise ratio in the double-prism spectrometer is approximately 200, while the pyro-electric sensors in CRISP4 are approaching their sensitivity limit, especially below approx. 10  $\mu$ m.

At  $\lambda = 8.77$   $\mu$ m, a transition from the first to the second grating stage is visible in the CRISP4 signal [3]. The discontinuity in the CRISP4 trace can indicate an alignment issue. This is currently under investigation, as well as the discrepancy for wavelengths above 14  $\mu$ m, where bulk absorption of zinc selenide has a significant contribution to the response function.

The bunch charges, measured with an integrated current transformer (ICT), are 232 pC (setting 1) and 146 pC (setting 2). The measurements have been taken at an electron beam energy of 970 MeV.

## SUMMARY AND OUTLOOK

In this contribution, we present a double-prism spectrometer suitable for the longitudinal diagnosis of femtosecond electron bunches. The spectrometer is equipped with sensitive detectors extending a high signal-to-noise ratio to mid-infrared wavelengths. In combination with the double-prism design, the setup enables a single-stage measurement of coherent transition radiation in the wavelength range between 2  $\mu$ m and 18  $\mu$ m in a single shot.

The spectrometer has been set up and commissioned at the transition radiation source at FLASH at DESY. The results are in agreement with measurements of established

diagnostics. A quantitative calibration in wavelength and intensity is currently in preparation.

Thus, the spectrometer is qualified to face the challenges imposed by conventional and novel concepts of particle accelerators, both yielding bunch charges in the sub-10 pC regime and lengths below ten femtoseconds.

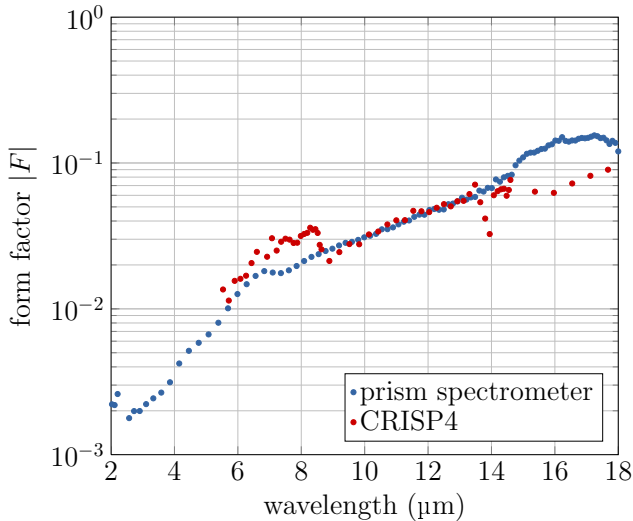


Figure 5: Comparison of the form factors at compression setting 1.

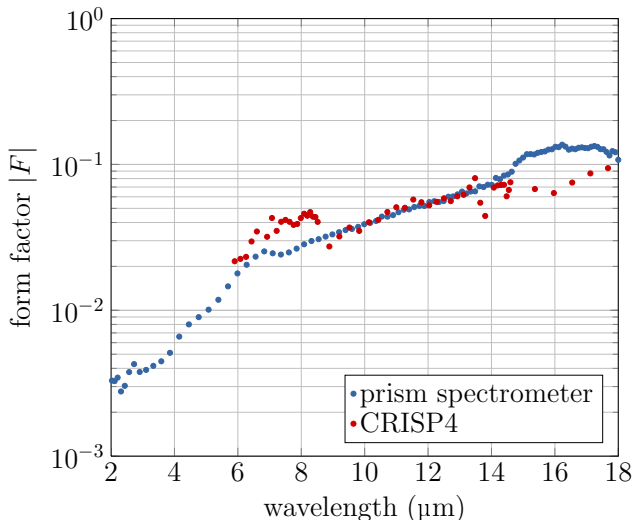


Figure 6: Comparison of the form factors at compression setting 2.

## REFERENCES

- [1] J. Rönsch-Schulenburg et al., Proceedings of FEL 2014, TUB04 (2014), to be published
- [2] O. Lundh et al., Nature Physics 7, 219–222 (2011)
- [3] S. Wesch et al., NIM A 665 (2011) 40–47
- [4] E. Hass et al., Proceedings of IBIC 2013, MOPC37 (2013)
- [5] R. Lai et al., NIM A, 397, 221–231 (1997)
- [6] D. Pelliccia and T. Sen, “A two-step method for retrieving the longitudinal profile of an electron bunch from its coherent radiation”, ArXiv preprint 1403.1233v1 (2014)
- [7] S.I. Bajlekov, Phys. Rev. ST Accel. Beams 16, 040701 (2013)
- [8] O. Zarini and A. Debus et al., DPG-Frühjahrstagung, Göttingen (Poster), T 129.17 (2013)
- [9] T.J. Maxwell et al., Phys. Rev. Lett. 111, 184801 (2013)
- [10] P. Norton, Opto-Electronics Review 10 (3), 159–174 (2002)
- [11] InfraRed Associates, <http://www.irassociates.com/>
- [12] L.S. Rothman et al., Journal of Quantitative Spectroscopy & Radiative Transfer 130 (2013) 4–50
- [13] B. Schmidt, Proceedings of FEL 2006, THCAU01 (2006)
- [14] J.R. Schneider, Journal of Physics B 43, 194001 (2010)
- [15] S. Casalbuoni et al., Phys. Rev. ST Accel. Beams 12, 030705 (2009)
- [16] V. Balandin et al., “Studies of the Collimator System for the TTF Phase 2”, TESLA report 2013-17 (2013)
- [17] C. Behrens and C. Gerth, Proceedings of FEL 2010, MOPC08 (2010)